AWARD NUMBER: W81XWH-15-1-0390

TITLE: Theranostics Targeting Metastatic Breast Cancer

PRINCIPAL INVESTIGATOR: Zheng Li

CONTRACTING ORGANIZATION: Methodist Hospital
Houston, TX 77030

REPORT DATE: October 2017

TYPE OF REPORT: Annual

PREPARED FOR: U.S. Army Medical Research and Materiel Command
Fort Detrick, Maryland 21702-5012

REPORT DOCUMENTATION PAGE

Form Approved
OMB No. 0704-0188

1. REPORT DATE	2. REPORT TYPE	3. DATES COVERED
October 2017	Annual	30 Sep 2016 - 29 Sep 2017

4. TITLE AND SUBTITLE

Theranostics Targeting Metastatic Breast Cancer

5a. CONTRACT NUMBER

5b. GRANT NUMBER
W81XWH-15-1-0390

5c. PROGRAM ELEMENT NUMBER

6. AUTHOR(S)

Zheng Li

Email: zli@houstonmethodist.org

5d. PROJECT NUMBER

5e. TASK NUMBER

5f. WORK UNIT NUMBER

7. PERFORMING ORGANIZATION NAME(S) AND ADDRESS(ES)
.
Methodist Hospital
Houston, TX 77030

8. PERFORMING ORGANIZATION REPORT NUMBER

9. SPONSORING / MONITORING AGENCY NAME(S) AND ADDRESS(ES)
U.S. Army Medical Research and Materiel Command
Fort Detrick, Maryland 21702-5012

10. SPONSOR/MONITOR'S ACRONYM(S)

11. SPONSOR/MONITOR'S REPORT NUMBER(S)

12. DISTRIBUTION / AVAILABILITY STATEMENT
Approved for Public Release; Distribution Unlimited

13. SUPPLEMENTARY NOTES

14. ABSTRACT
The emphasis of this first year of the award, as planned, has been on synthetic chemistry to obtain materials to test in histology, PET (positron emission tomography) and PDT (photodynamic therapy) studies. We have been successful in preparing samples for the testing studies that begin in year 2. However, as anticipated, the synthetic chemistry work was not without problems and must continue and adapt to overcome challenges that now become evident. For instance, one of the molecules first prioritized, compound 1, was prepared, but only after a great deal of effort; in retrospect it is now clear that this compound has stability issues that make it hard to make, and inappropriate for further studies. Another target compound (2) was then prepared, much more efficiently than the first because it does not have stability issues, and because of the experience we gained from making the first target. This compound has poor solubility characteristics despite the fact that it contains two sulfonic acid groups and may required delivery in micelles; this is something that could not have been predicted until the compound was made. Both structures 1 and 2 are based on the aza-BODIPY dye fragment; as a back-up we have also initiated work on a compound based on a different-dye type, eg compound 3. The original proposal outlined plans to add cytotoxic entities other than PDT agents; for this we entered into a collaboration with a biotechnology company who have provided us a small sample of the previous, highly cytotoxic, compound maytensin A. We have also prepared an agent intended solely for PET, ie compound 4; this takes advantage of very recent advances in the field that enable more efficient capture of 18F- than was possible before, via so-called "Perrin capture agents.

15. SUBJECT TERMS-

Nothing listed

16. SECURITY CLASSIFICATION OF:			17. LIMITATION OF ABSTRACT	18. NUMBER OF PAGES	19a. NAME OF RESPONSIBLE PERSON
a. REPORT	b. ABSTRACT	c. THIS PAGE			USAMRMC
U	U	U	UU	21	19b. TELEPHONE NUMBER *(include area code)*

Table of Contents

Page

1. Introduction……. 4

2. Keywords……. 4

3. Accomplishments……..……... 4

4. Impact……...…… 11

5. Changes/Problems...…..…… 12

6. Products…….……..…..……. 12

7. Participants & Other Collaborating Organizations……. 13

8. Special Reporting Requirements…… 13

9. Appendices…… 14

Theranostics Targeting Metastatic Breast Cancer

A. Introduction (1paragraph)

The overall goal of this proposal is to prepare TrkC$^+$-targeted fluorescence/PET/PDT for breast cancer. For this we use a TrkC$^+$ targeting fragment (parts of structures colored in blue throughout this report) and compare them with isomeric compounds that do not target TrkC$^+$ (green). Last year we reported the synthesis aza-BODIPY **1**. This compound was designed for optical imaging of TrkC$^+$ tumors; this year we did that in a 4T1 mouse model, and published the results. Agent **1** accumulated well in tumors, but was not very bright perhaps due to insolubility aggregation effects. We had also proposed to make compound **2** for positron emission tomography (PET) and photodynamic therapy (PDT). After much effort, we made **2** then realized the reason that was so difficult was due to compound instability, specifically the compound loses iodine easily. Instability means **2** is not useful for imaging or therapy. Consequently, just as indicated as a back-up plan last year, we switched focus to the more water-soluble cyanine-based systems (here, **3** - **7**). These are more soluble, brighter, and less prone to aggregation. So far, dyes **3** and **4** have been tested *in vivo*, but they accumulated in the kidneys and cleared quickly with little imaging of the tumor. To address this issue, we have prepared other systems with more lipophilic cyanines (*eg* **5** - **7**), and plan to make other systems with albumin binders to increase retention (based on a literature precedent); all these compounds are ready to be tested *in vivo*. It is necessary to find cyanines that sensitize production of singlet oxygen to realize the overall goal of this study: fluorescent/PET/PDT theranostics. We discovered a brominated cyanine core that does indeed act as a singlet oxygen sensitizer, and compounds **5** – **7** are designed to exploit this. Finally, we prepared the targeted PET agent (**8**), and the targeted maytensin (**9**) mentioned in our previous report (also awaiting *in vivo* studies). The PET agent **8** was tested *in vivo* in a 4T1 mouse model; it had good stability (no 18-fluoride in bone) but cleared quickly. Modifications of this are suggested for year 3.

B. Keywords (limit to 20 words)

reagents for histology of TrkC$^+$ tumors • photodynamic therapy (PDT) • positron emission tomography (PDT)

C. Accomplishments

What were the major goals of the project?

1 Design and synthesis of second-generation fluorescent, PDT and PET/PDT agents *that absorb >700 nm*, bind TrkC, are localized in TrkC$^+$ cells, generate singlet oxygen under conditions for PDT, and have TrkC$^+$ selective photocytoxicities.

begins in year 1 and continues throughout grant period (about 40 % of total work required achieved this year)

2 Validation of a fluorescent form of one of these agents in histochemistry for diagnosis of patients with TrkC$^+$-expressing tumors.

year 2 and then continues throughout grant period

3 Validation of the iodinated second-generation agent PET imaging human breast cancer tumors in mice, and ablation of these tumors via PDT. This study will involve determination of toxicity *in vivo*, pharmaco-kinetics and -dynamics (using PET) to ascertain distribution and clearance of the labels.

only in years 2 and 3

What was accomplished under these goals?

Optical Imaging With Compound **1**

Compound **1** (and the non-targeting, isomeric control, not shown) were tested in the *in vivo* mouse 4T1 model, and the results are summarized below. This study was successful, good accumulation in the tumor was obtained. (Kamkaew A., Li F, Li Z.* and Burgess K*. An agent for optical imaging of TrkC-expressing, breast cancer. Med. Chem. Commun., 2017,8, 1946-1952)

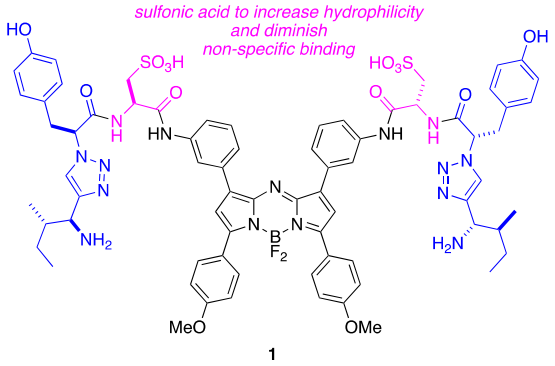

1

a

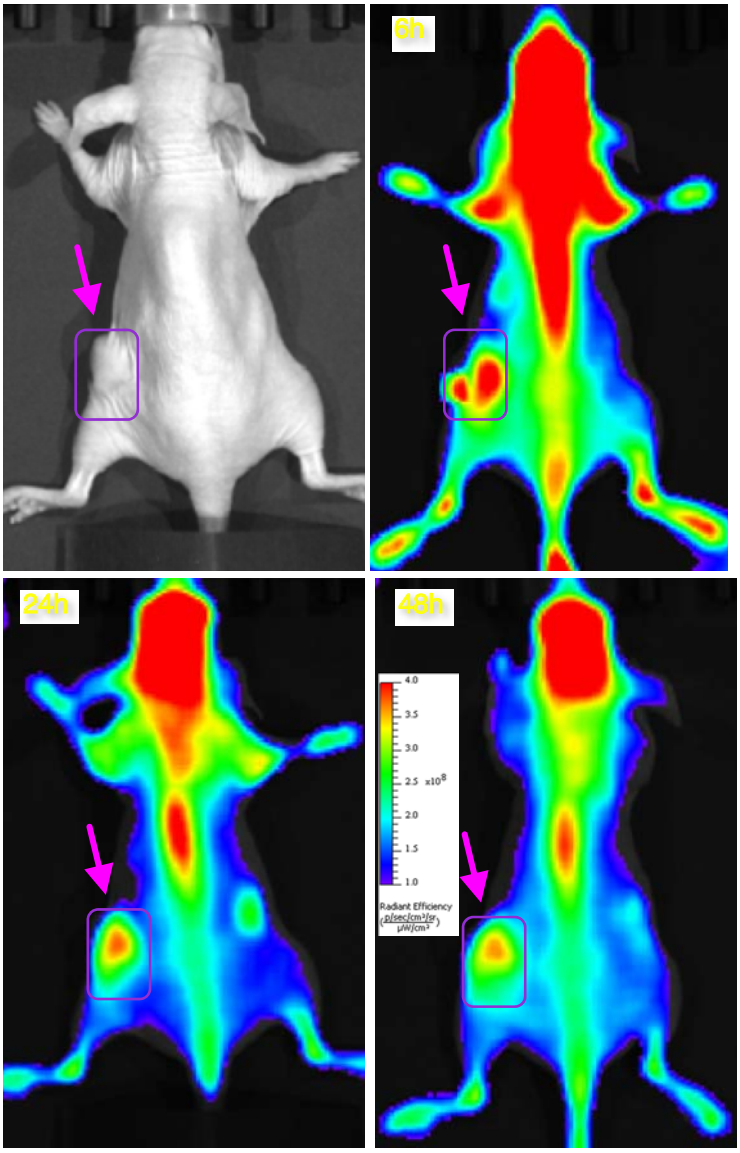

b

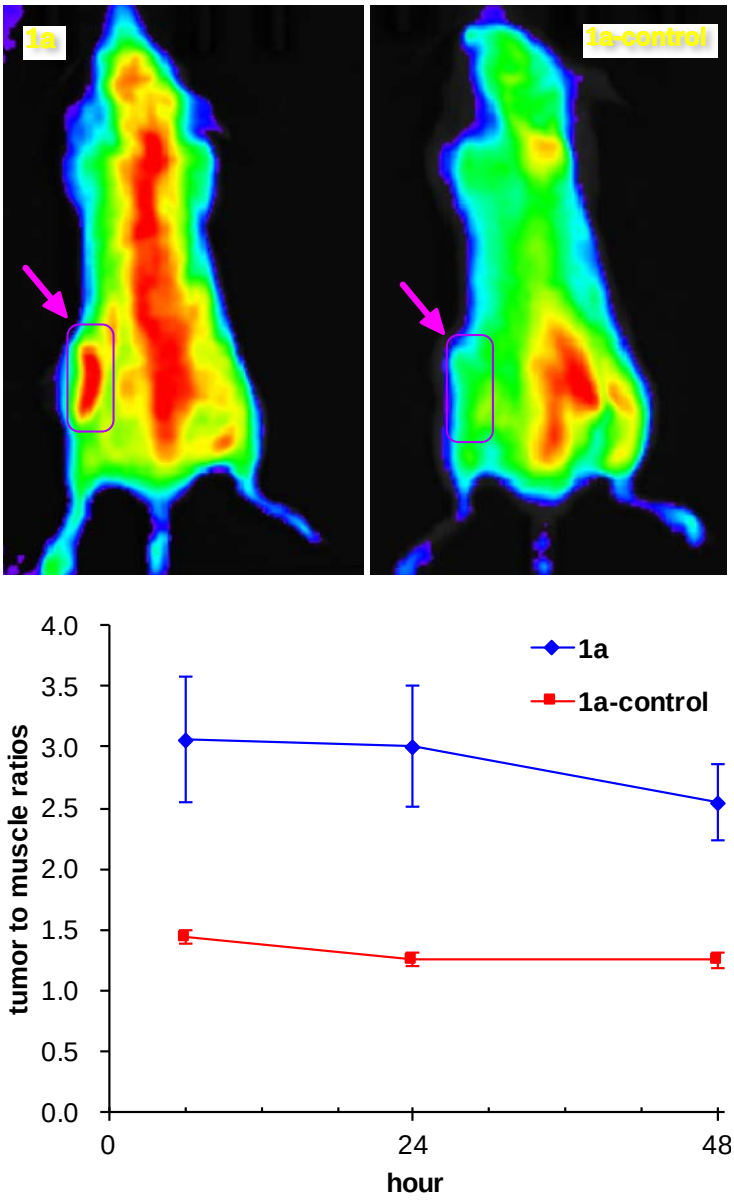

Figure 1. **a** *In vivo* NIR fluorescence images (at 6 h, 24 h, and 48 h p.i.) of 4T1 tumor-bearing mice injected (iv) with **1a**. Arrows indicate the tumors. **b** Representative NIR fluorescent images of mice injected with **1** (left) or **1-control** compound at 48h p.i. (right). The arrows indicate the tumors (top); a region of interest (ROI) study of tumor/normal tissue (muscle) ratio of **1a** and **1-control** in the imaging groups (n = 3).

The corresponding iodinated aza-BODIPY **2** was unstable (see below) hence this aza-BODIPY approach could not lead to the integrated fluorescent/PET/PDT theranostic that we are determined to prepare. Consequently, this approach was abandoned in favor of ones featuring cyanine dyes. We felt the superior solubility of select cyanine dyes would reduce aggregation, and increase brightness in optical imaging studies. Moreover, it is easier to design cyanines that absorb over 750 nm than it is for aza-BODIPYs.

Compound **2** Intended For PET and PDT Imaging

Compound **2** (and the corresponding control). These syntheses are about 10 steps, and the final product kept decomposing making us think the reactions to form it had failed. Agent **2** is *not* a good approach to the theranostic, and we regret spending so much time on this.

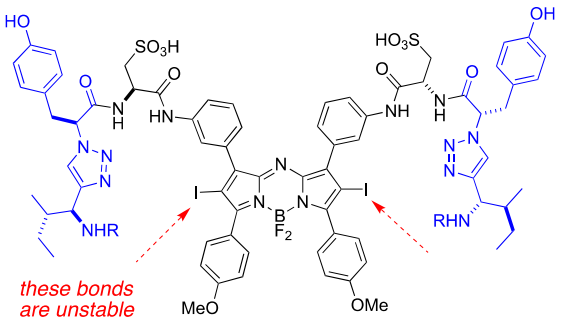

2

Change of strategy to the cyanine dyes was important; and this has been much more fruitful, though not without set-backs.

Investigation Of Cyanine Systems **3** and **4** For Optical Imaging

We prepared systems **3** (and the control indicated), and obtained photphysical properties for these agents. These cyanines absorb around 760 nm and fluoresce with a maximum of around 790 nm, which is ideal for optical imaging *in vivo*. In cell studies on a high-power fluorescent microscope we can see that the targeted dye **3** has a higher affinity to NIH 3T3 TrkC$^+$ transfectant cells than the control. However, because of filter issues, we are currently not able to image live cells treated with these agents on our confocal apparatus (we are trying to vary conditions to correct this). In histology, however, **3** stains metastatic breast cancer much more efficiently than the control **3-control**.

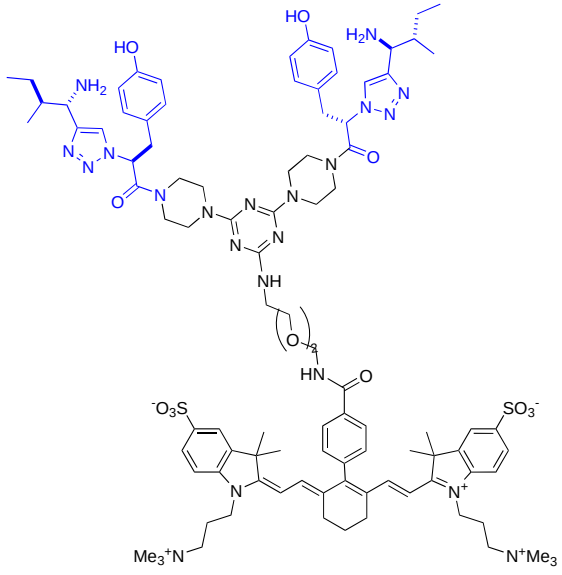

IY-IY-Targeted Cyanine

3

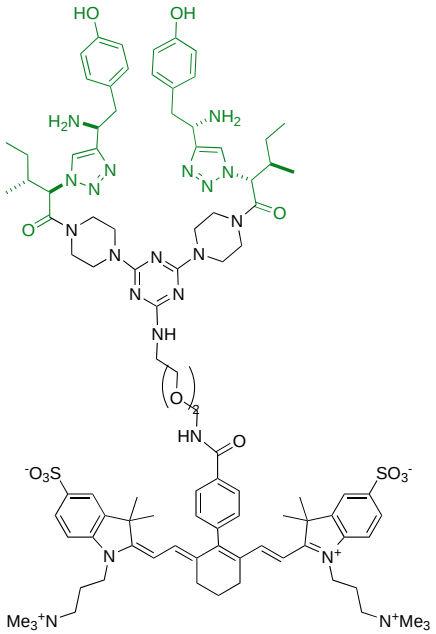

YI-YI (Non-targeted Cyanine)

3-control

Optical imaging of these compounds was performed in the 4T1 murine model, and in another TrkC^{+}, Hs578t implanted into nude mice (better image since these mice have no hair). The data (Fig 1) show these agents were not retained well; they accumulated in the kidneys and were cleared rapidly.

a

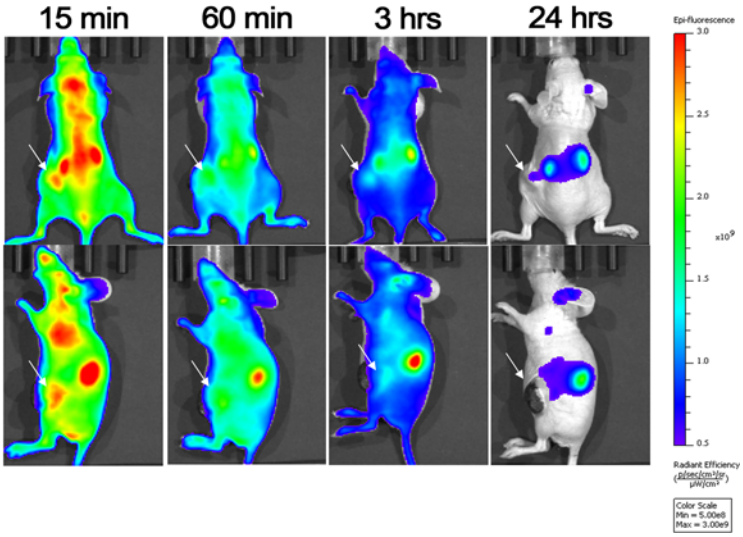

b

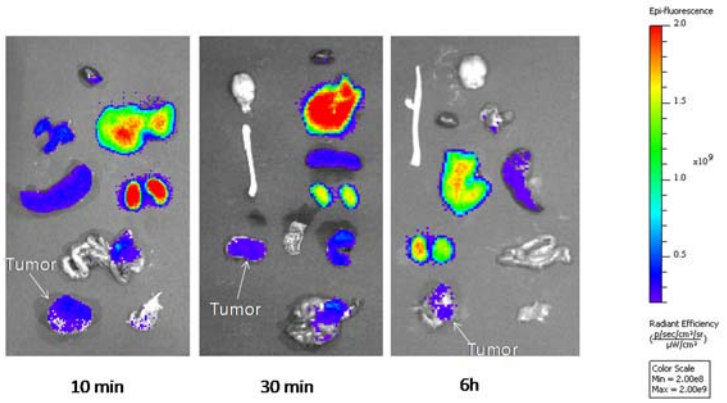

Figure 1. **a** Optical imaging of probe KB2251 in 4T1 breast cancer bearing mice (n=3). Murine 4T1 cancer cells with TrkC expression were inoculated into nu/nu mouse to create breast cancer animal model. Probe KB2551 (5 nmol/mouse) was injected via tail vein, and in vivo optical imaging was captured with an IVIS200 imaging system and quantified by Living Imaging software (Xenogen, Alameda, CA). Images were acquired at 15mins, 60mins, 3 h, and 24 h postinjection (p.i.). Excitation and emission filters were set at 745 and 800 nm respectively as suggested by the system for image acquisition. Tumors are indicated by arrowheads. Tumor uptake was clearly visualized at early time point but the probe is very highly hydrophilic and is washed out quickly. High kidney uptake at early time point and rapidly decreased demonstrating a fast renal excretion. From this result, new probe with an Albumin binder is designed for increasing the circulation time, the next generation compound will be prepared by Dr. Burgess's lab following the in vitro and in vivo validation. **b** Biodistribution study of KB2251 compound in 4T1 breast cancer bearing mice. Tumors and other major organs (i.e., liver, spleen, kidney, heart, lung, brain, spinal cord and intestines) were dissected intact upon immediately sacrificing the mice at 10min, 30min and 6h. White arrow marks the tumor.

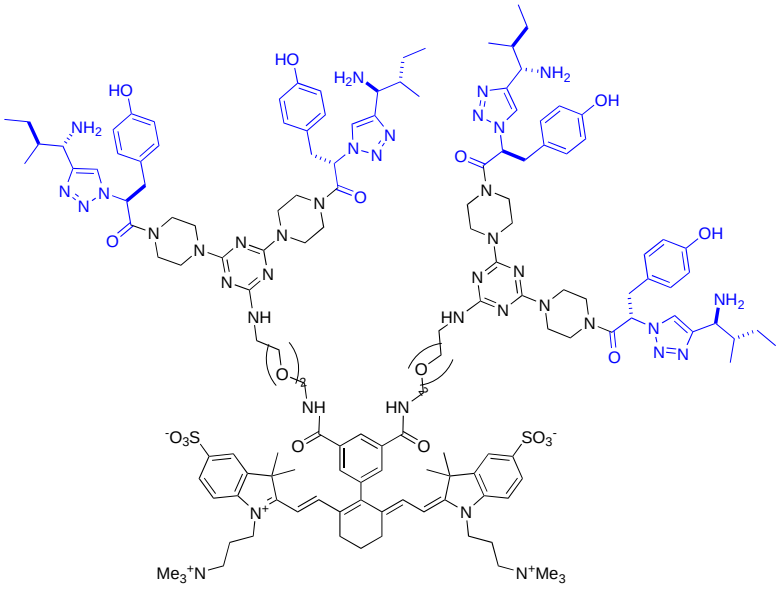

IY-IY (Targeted Cyanine)

4

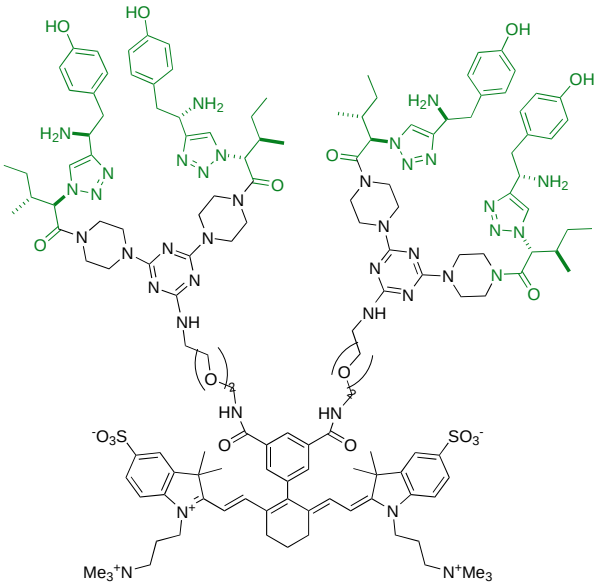

YI-YI (Non-targeted Cyanine)

4-control

We also prepared compounds **4** and **4-control** suspecting that these molecules having *two* IY-IY binding groups would have an even higher affinity for cells expressing TrkC$^+$. In the event, this appeared to be true in live cell staining. However, for reasons we currently do not understand, *in vivo* these compounds were *less* visible in nearIR imaging.

Our conclusions from these studies are that the dye should be made more lipophilic or should be modified to incorporate an albumin binding molecule (based on literature precedent).

More Lipophilic Cyanine Systems That Should Be Cleared More Slowly

Compounds **5** and **6** were designed to have cyanine dyes that are less hydrophilic than **3** and **4**. So far we have determined that these systems do indeed bind NIH 3T3 TrkC$^+$ transfectant cells, and metastatic breast cancer in histology experiments. The water-solubilities of these systems were also determined. We have not yet been able to determine a K_d for these compounds binding the TrkC$^+$ receptor because there is no obvious "blocking group' for in cells studies; however, we continue to search for a work-around to this problem.

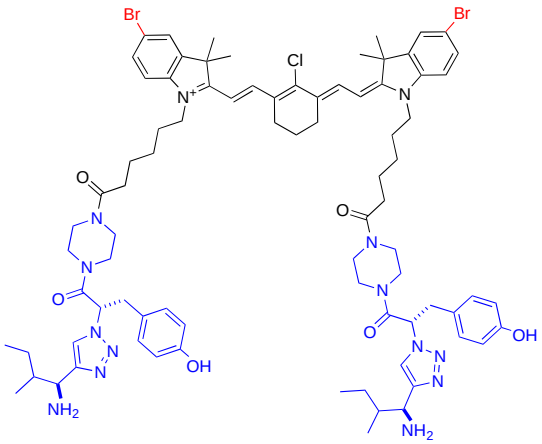

5

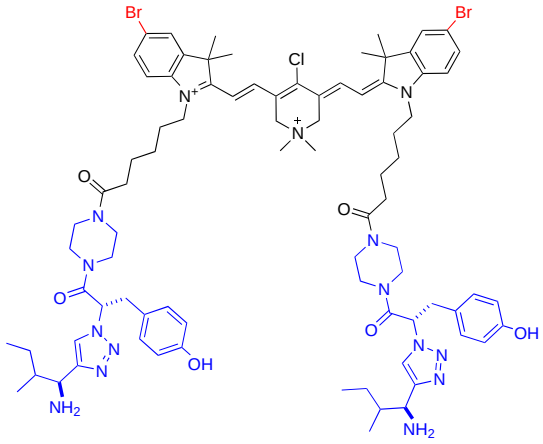

6

Compounds **5** and **6** have the potential to be near-IR imaging agents and PDT therapeutics *in vivo* (see below). They will be tested in this upcoming research year.

Cyanine Dyes In PDT

It transpires that relatively little is known about cyanine dyes in PDT; there have been only a few studies. We found that the parent dibromide cyanines from which **5** and **6** are made are good PDT agents. While these experiments were in progress another group reported PDT studies on very similar {untargeted} diiodide systems. The *in vivo* work alluded to above should be extremely interesting; it may be the first targeted study with cyanine dye sensitizers.

Potential Fluorescent/PET/PDT Theranostic **7**

We have also prepared compound **7** which could become our lead theranostic. This structure has the TrkC^{+} targeting group (blue), a Perrin ^{18}F capture unit (purple) and a PDT active cyanine backbone: all the components for a fluorescent/PET/PED theranostic. Currently we are scaling up the synthesis of this molecule, for photophysical measurements, cellular assays particularly light/dark cytotoxicity, then *in vivo* studies.

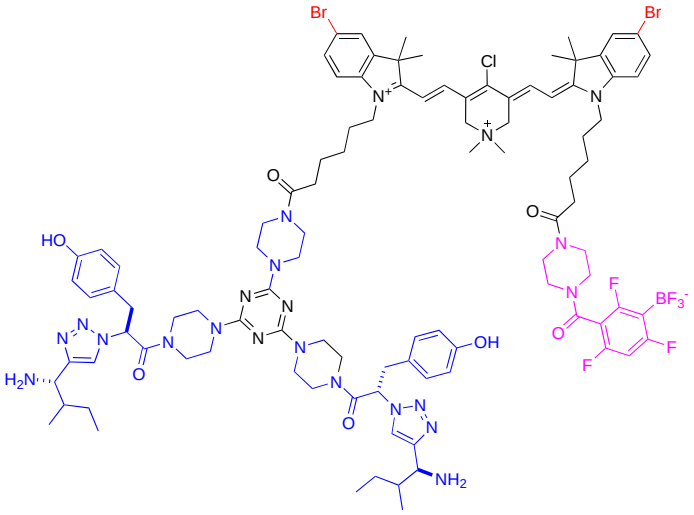

7

Targeted PET Label **8**

Our objective was to perform at least one set of PET experiments in year 2, consequently we made and tested the TrkC^{+} targeted PET agent **8**. Exchange of ^{19}F with ^{18}F was performed on this system with a 6 – 8 % radiochemical yield. Unfortunately, the pharmacokinetic properties of this agent were unfavorable because it cleared too rapidly. However, it dd not release ^{18}F *in vivo*; we know this because the label did not accumulate in the bone.

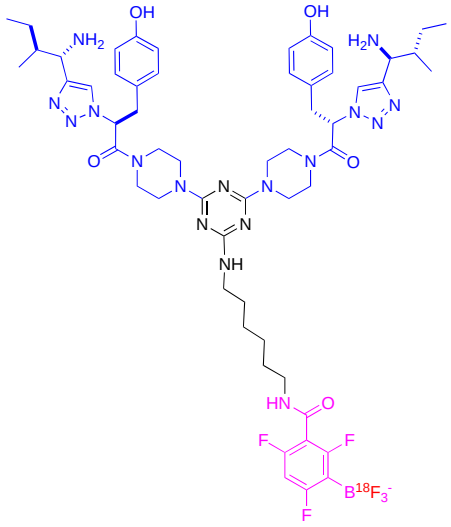

8

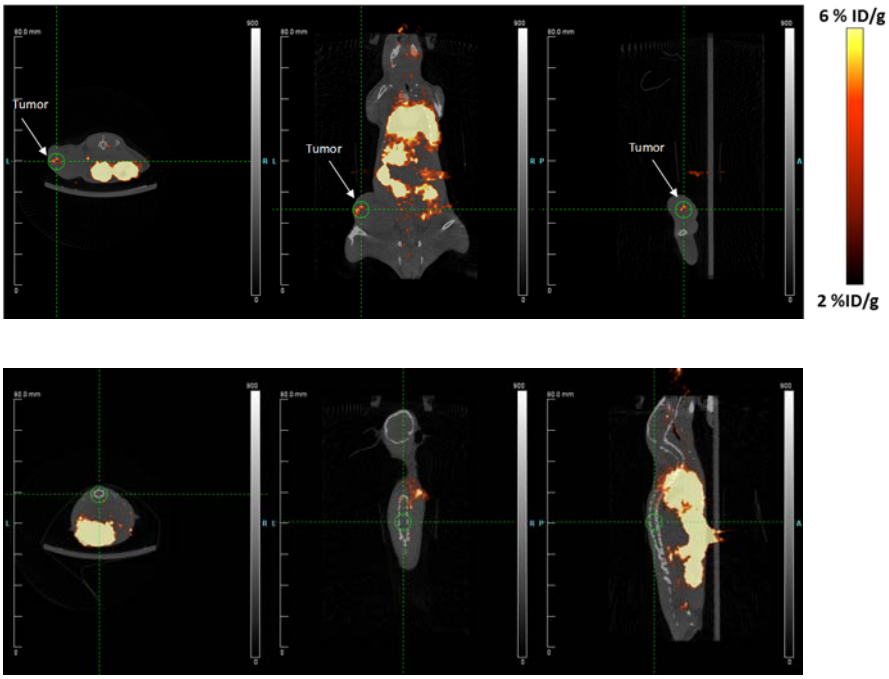

Figure 3. Small-animal PET/CT imaging of U-87 tumor-bearing mice. Small-animal PET/CT scans of 4T1 tumor–bearing mice injected intravenously with approximately 3.7 MBq of F-18 KB2265 at 10mins p.i. Tumors are indicated by arrowheads (top). There is no uptake in the bone and spinal cord indicating good in vivo stability of the F-18 KB2265 (bottom).

Targeted Maytensinoid Therapeutic **9**

Finally, in collaboration with a biotech company who donated the maytansinoid **DM4**, in out labs we prepared the targeted conjugate **8** equipped with a disulfide linker designed to be cleaved in the cytosol. Cell studies with agent **9** in comparison with **9-control** indicate there is slightly improved cellular therapeutic index. However, we expect the improvements to therapeutic index *in vivo* to be more profound because of pharmacokinetic effects that cannot be replicated in cell culture. This compound awaits *in vivo* studies.

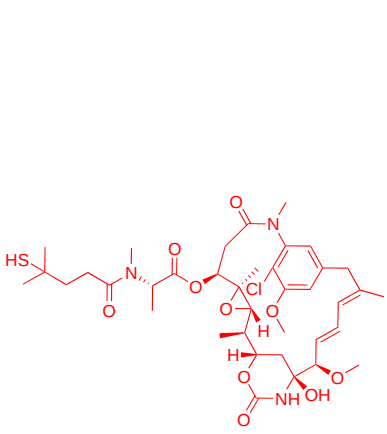

maytansinoid DM4

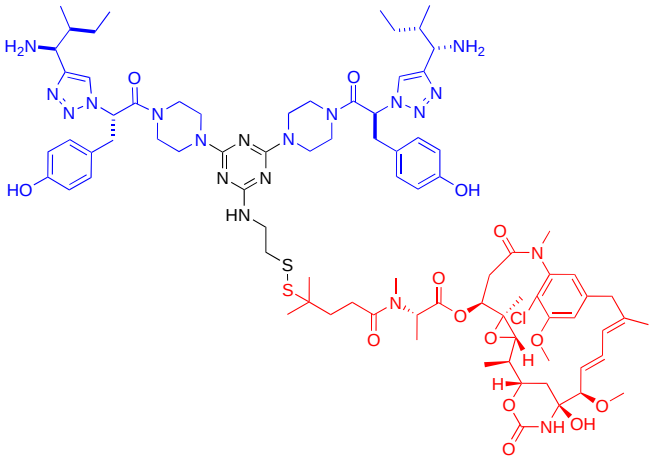

9

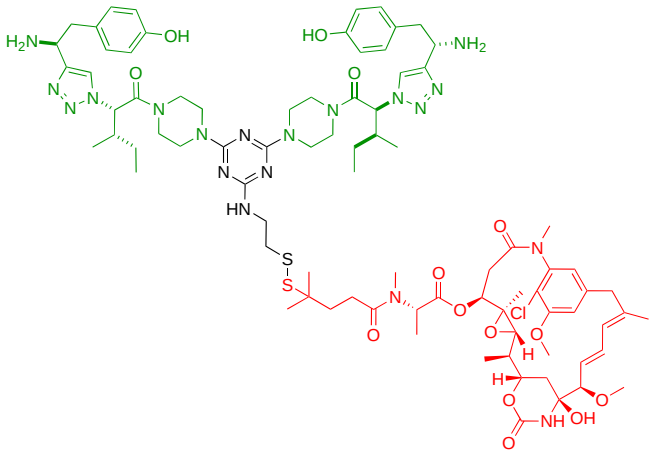

9-control

What opportunities for training and professional development has the project provided?

This funding has been used to support post doctoral fellow Jaya Shrestha, and graduate students Usama Syed, Bosheng Zhou, and Daniel Jiang.

What do you plan to do during the next reporting period to accomplish the goals?

During the next reporting period we will:

(i) initiate *in vivo* studies (PDT and PET) on some of the compounds already prepared; and,

(ii) continue the synthetic studies to produce agents with superior solubility and PDT characteristics.

D. Impact

What was the impact on the development of the principle(s) of the project?

Optical imaging of TrkC targeting probe has been developed and the result have been published recently. PET imaging study is ongoing and we'll start PDT therapy study soon.

What was the impact on other disciplines?

Too early to impact other disciplines.

What was the impact on technology transfer?

A patent application is still in process for the IY-IY targeting groups.

What was the impact on society beyond science and technology?

Too early to impact society outside science, but eventually the goal of this work is to produce a lead compound that will be iteratively improved to form a "theranostic" for diagnosis, imaging, and therapy.

E. Changes/Problems

Changes in approach and reasons for change

Actual or anticipated problems or delays and actions or plans to resolve them

Problems are nearly always encountered in chemical syntheses, but we have anticipated the obvious weak links and constantly consider alternative routes.

If the solubility of compound **2** is insufficient, we plan to deliver it in a micellular system.

Changes that had a significant impact on expenditures

Postdoctoral salaries are more than before as a result of the new labor laws. This will be a problem going forward, but it has not been a problem so far.

Significant changes in use or care of human subjects, vertebrate animals, biohazards, and/or select agents

none

Significant changes in use of care of human subjects

n/a

Significant changed in use of care of vertebrate animals

none

Significant changes in use of biohazards and/or select agents

none

F. Products

Publications, conference papers, and presentations

Kamkaew A., Li F, Li Z.* and Burgess K*. An agent for optical imaging of TrkC-expressing, breast cancer. Med. Chem. Commun., 2017,8, 1946-1952

Websites or other Internet sites

none

Technologies or techniques

Only the novel syntheses already described.

Inventions, patent application, and/or licenses

A patent application covering the targeting ligands is still in progress.

Other Products

none

G. Participants & Other Collaborating Organizations

What individuals have worked on the project?

(for each individual please give a brief description of their contribution to project and how many months they worked on the project)

Dr. Feng Li (research associate) 50% (6 months): synthesis and radiolabeling, in vitro stability study, imaging study

Dr. Zhen Yang (postdoc fellow) 100% (Hired in the end of May 2017, 5 months working on this project so far): Animal model, cell study, imaging study and future PDT therapy study

Has there been a change in the active other support of the PD/PI(s) or senior/key personnel?

What other organizations were in involved as partners?

Dr. Kevin Burgess in Texas A&M

Special Reporting Requirements

none

H. Appendices (attached journal articles, reprints, CV, patent applications)

MedChemComm

RESEARCH ARTICLE

View Article Online
View Journal

Cite this: DOI: 10.1039/c7md00328e

An agent for optical imaging of TrkC-expressing, breast cancer†

Anyanee Kamkaew,[ab] Feng Li,[c] Zheng Li*[c] and Kevin Burgess *[a]

Tropomyosin receptor kinases receptor C is expressed at high levels on the surface of tumors from metastatic breast cancer, metastatic melanoma, glioblastoma, and neuroblastoma. Previous studies have shown synthetic TrkC ligands bearing agents for photodynamic therapy could be used to completely ablate 4T1 metastatic breast tumors and suppress metastatic spread *in vivo*. Modification of these probes (**A** in the text) to make them suitable for near infrared optical imaging *in vivo* would require a substantial increase in molecular mass (and hence increased vulnerability to undesirable absorption, metabolism and immunogenicity effects), or significant changes to the probe design which might compromise binding to TrkC in histochemical studies and on live cells. The research featured here was undertaken to investigate if the second strategy could be achieved without compromising binding to TrkC-expressing tissues. Specifically, an "aza-BODIPY" probe was synthesized to replace a spacer fragment in the original probe **A**. In the event, this new probe design (**1a** in the text) binds TrkC$^+$ breast cancer in live cell cultures, in histochemical studies and in an *in vivo* murine model. Probe **1a** binds TrkC$^+$ tissues with good contrast with respect to healthy tissues, and much more strongly than an isomeric, non-TrkC binding, probe (**1b**) prepared as a negative control.

Received 28th June 2017,
Accepted 17th August 2017

DOI: 10.1039/c7md00328e

rsc.li/medchemcomm

Introduction

Tropomyosin receptor kinases (Trk's) are cell-surface receptors that bind the neurotrophin growth hormones.[1] Docking neurotrophin-3 (NT3) with TrkC, for instance, triggers intracellular phosphorylation then a network of cell signaling processes that lead to cell growth and differentiation.[2,3] Overexpression of Trk receptors is associated with several forms of cancer, including neuroblastoma,[4–16] glioblastoma,[14,17–21] metastatic breast cancer[22–28] and metastatic melanoma.[29–37] Consequently, functionalized Trk ligands may be prepared as possible imaging agents for cancer.[28,38–40] Synthetic TrkB-[41] and pan-Trk-binding agents[16] functionalized with radionuclei have been explored for imaging with positron emission tomography (PET), but, to the best of our knowledge, no synthetic imaging agents have been reported for selective optical-imaging of TrkC *in vivo*.

Prior research from these laboratories featured the TrkC-homing ligand in structure **A**. Probe **A** was shown to be internalized by TrkC-expressing cells and it could also be used as a staining agent for metastatic breast cancer and melanoma tissue, both of which are associated with TrkC overexpression. Moreover, one 10 mg kg^{-1} dose of **A** coupled to a BODIPY-based PDT agent was shown to almost completely ablate a 4T1 primary tumor, and suppress metastatic spread.[42]

Probe **A** is not ideal for optical imaging because it absorbs light optimally at a wavelength (around 500 nm) that is too short for efficient penetration of more than a few mm in tissue.[43,44] To circumvent this, the most obvious solution would be to prepare similar molecules with a near-IR-absorbing probe directly replacing the BODIPY. However, modifications to fluors to make them near-IR absorbing invariably increase their molecular size; this is undesirable because larger structures tend to be more vulnerable to undesirable absorption, metabolism, and excretion effects. We reasoned that one way to reconcile these opposing design criteria is to replace the black part of structure **A** with a near-IR fluor giving the generic structures **B** (Fig. 1). Designs **B** eliminate the triazine core which serves no purpose other than as a scaffold-spacer. One possibility would be to replace it with an aza-BODIPY dye; these dyes tend to have significantly longer absorption and emission wavelength maxima than their BODIPY analogs.[45–47]

[a] *Department of Chemistry, Texas A & M University, Box 30012, College Station, TX 77842, USA. E-mail: burgess@tamu.edu*
[b] *School of Chemistry, Institute of Science, Suranaree University of Technology, Nakhon Ratchasima 30000, Thailand*
[c] *Center for Bioenergetics, Houston Methodist Research Institute, Houston, TX 77030, USA. E-mail: zli@houstonmethodist.org*

† Electronic supplementary information (ESI) available: Scheme and full details of compounds syntheses and characterizations, cell toxicity of **1a** and TrkC antibody stained on breast tissues. See DOI: 10.1039/c7md00328e

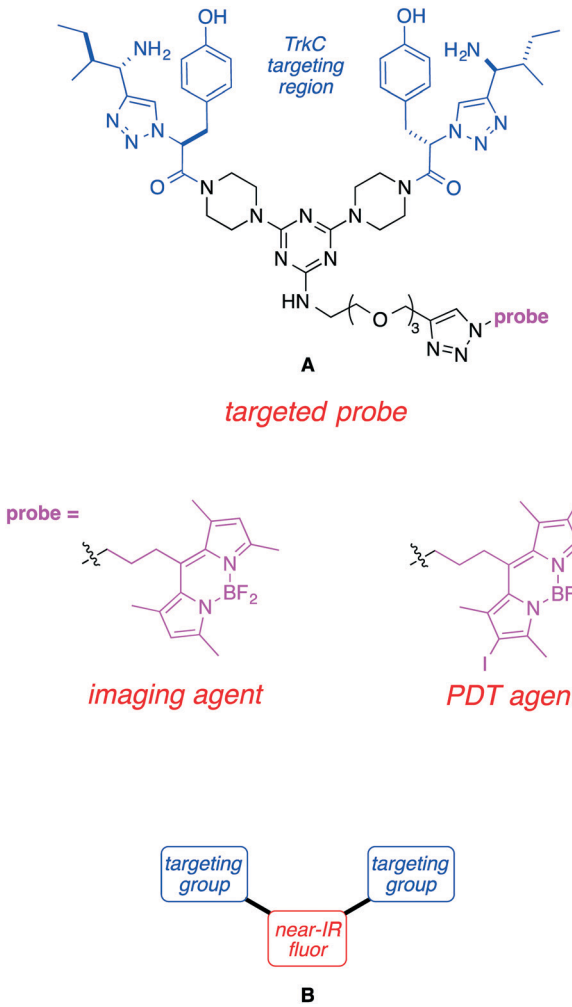

Fig. 1 First generation TrkC targeting ligand-conjugate **A** and the design concept in this paper **B**.

Based on the considerations outlined above, we designed aza-BODIPY dyes **1a** and **b** (Fig. 2). Probe **1a** was appealing because the sulfonic acid groups would enhance the hydrophilicity of the molecule and their negative charge might reduce non-specific binding to cells. Conversely, **1b** has the advantages of smaller size, and more facile synthetic access. We anticipated the best of these two probe candidates, based on solubility and spectroscopic experiments, would be tested for: (i) binding and internalization by TrkC-expressing cells; (ii) staining TrkC-expressing fixed tissue (histochemistry); and, (iii) comparative distribution in healthy mice and ones bearing TrkC-expressing breast cancer.

Results and discussion

Probe syntheses

Coupling of the azido acid from L-tyrosine[48] with the disulfonated aza-BODIPY **2**, prepared as described,[49] gave the diazide **3** (Scheme 1). A copper-mediated cycloaddition[50,51] of **3** with the alkyne derived from L-isoleucine[48] gave the desired product **1a**. Probe **1b** was prepared *via* an analogous route, but beginning with a diamine aza-BODIPY precursor to **2**; a scheme and full details of that synthesis are given in the ESI.†

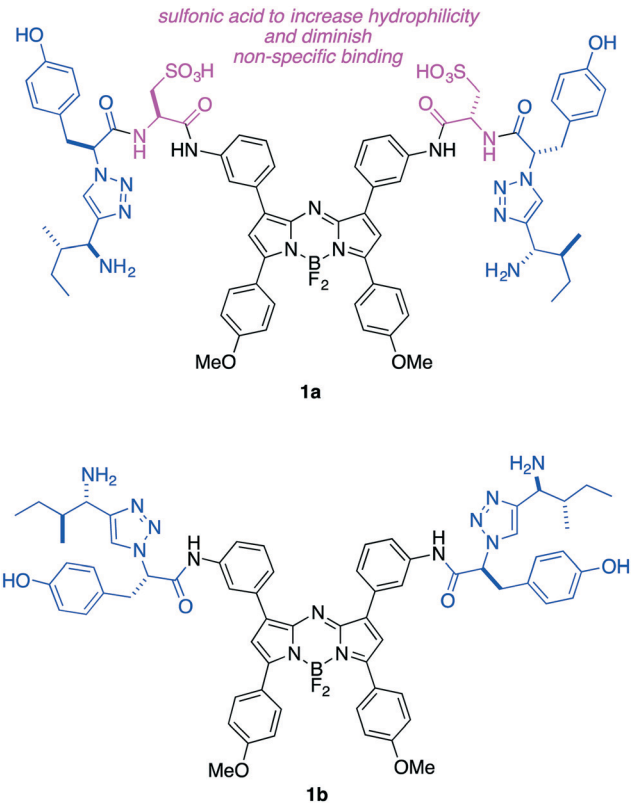

Fig. 2 Second generation TrkC targeting ligands **1a** and **1b** featured in this work.

Distribution of probes 1a and b in TrkC$^+$ murine breast cancer cells

TrkC-expressing, 4T1 murine breast cancer cells were treated with probes **1a** and **b**. Confocal microscopy (Fig. 3a) showed the sulfonated system **1a** was efficiently internalized whereas the more lipophilic system **1b** had poor solubility and appeared to give significantly more cell-surface binding (Fig. 3b). For both probes, the material that was internalized overlaid with a lysosome tracker, indicating it accumulated in that organelle. These data support the assertion that the sulfonic acid groups of **1a** reduce non-specific binding to TrkC$^+$ cells relative to the neutral probe **1b**, as expected because of repulsion between the negatively charged sulfonic acids and polar head groups at the cell surface.[52] Probe **1a** showed no sign of toxicity to 4T1 cells at concentrations up to and including 25 μM (Fig. S1†). All the subsequent work in this research was focused on **1a**, and studies of **1b** were discontinued, because these data indicate **1a** may have better characteristics for non-specific binding.

Histochemistry

Commercial samples of fixed human tissue from patients with stage 1, 2, and 3 malignant breast cancer were

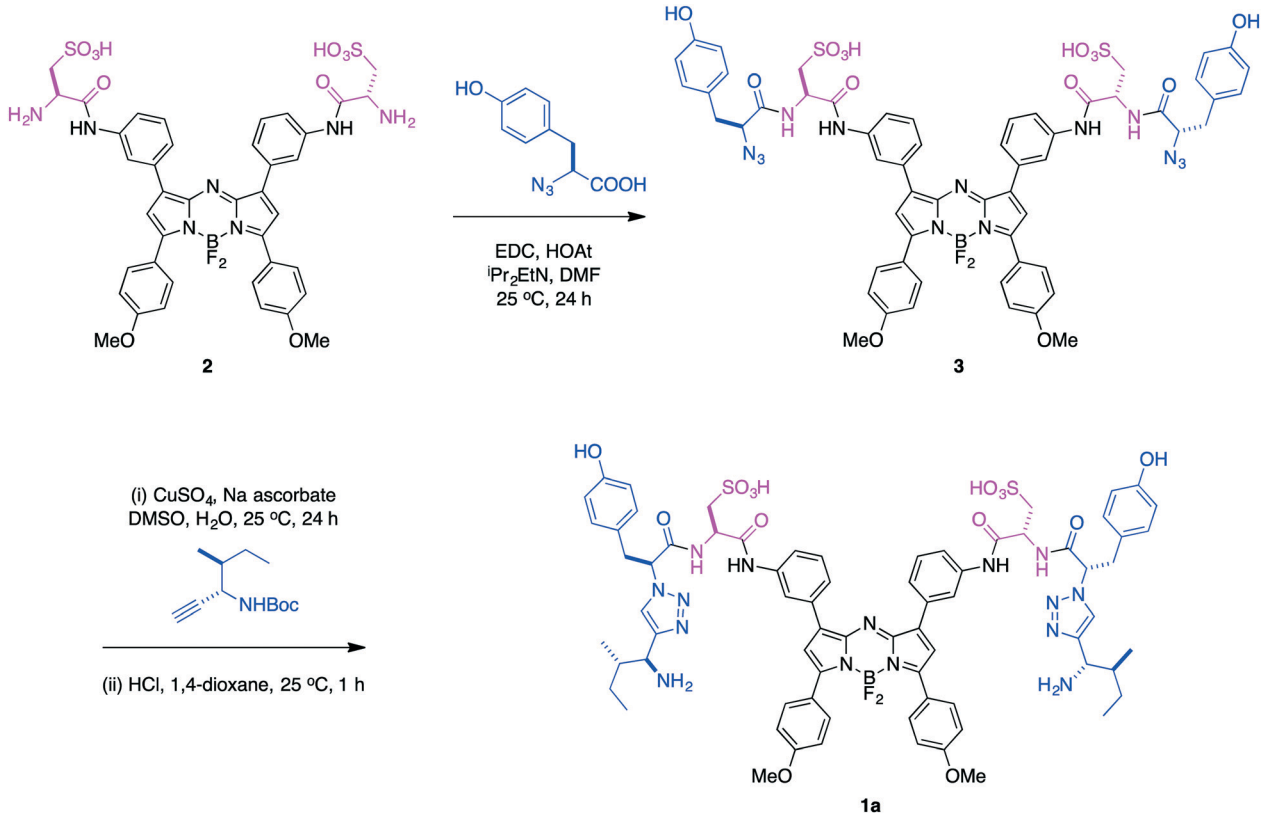

Scheme 1 Preparation of TrkC-targeted near IR probe **1a**.

purchased (US Biomax). Probe **1a** was used to treat these samples and the staining was compared to that observed for normal breast tissue proximal to the tumor, obtained from the same patient in each case; illustrative data are shown in Fig. 4. In all cases the tumor tissue stained strongly whereas the healthy samples showed much less fluorescence. We were encouraged by the selectivity, but slightly surprised that the healthy tissue showed faint staining. It appears that this is genuine binding to the TrkC receptor in the healthy tissue (rather than non-specific binding or fluorescence leakage into the red channel) because fluorescently labeled TrkC mAb also stained weakly the normal tissue (Fig. S2†). This may mean the tumor environment is causing the surrounding normal tissue to upregulate TrkC expression.

Optical imaging with 1a *in vivo*

A 4T1 breast cancer xenograft model was used (female BALB/c nu/nu mice, 8–10 mm diameter 4T1 tumors, *iv* administration) to evaluate **1a** as an *in vivo* optical imaging probe. Fig. 5 showed the NIR fluorescence images of nude mice bearing orthotopic 4T1 tumors after intravenous injection of 10 nmol of **1a**. The 4T1 tumors were clearly visualized with good tumor to background contrast at all time points (6, 24 and 48 h). As reported, Trk receptors are a family of tyrosine kinases that regulates synaptic strength and plasticity in the mammalian nervous system. TrkC is ordinarily activated by binding with NT-3 and is expressed by proprioceptive sensory.[53] We observed high uptake of **1a** in central nervous system (CNS) which correlated with the expression of TrkC receptor.

To validate the TrkC targeting specificity of **1a**, the scrambled negative control, **1a-control**, was prepared (structure in Fig. 6 and Scheme S2†) and tested for *in vivo* imaging and *ex vivo* studies (Fig. 5 and 6). 4T1 tumor uptake of the negative control was much lower at all time points comparing to **1a**, which confirmed the specific TrkC targeting. As shown in Fig. 5b, the tumor/normal tissue fluorescent signal ratios in the imaging group were 3.06 ± 0.88 at 6 h, 3.01 ± 0.85 at 24 h, and 2.54 ± 0.55 at 48 h p.i., respectively, which is 2–3 times higher than that of the control group (1.44 ± 0.09 at 6 h, 1.26 ± 0.08 at 24 h, and 1.21 ± 0.19 at 48 h p.i.).

Ex vivo imaging was performed to acquire the fluorescent images of internal organs for both imaging and control groups as shown in Fig. 6. The tumor fluorescent intensities in the imaging group (7.29 ± 0.67) are significantly higher than in the control group (1.52 ± 0.29), also confirming the specificity of the probe **1a** for TrkC. The average radiant efficiency of other organs in control group was similar to that of the imaging group.

Conclusion

Compounds **1a** and **1b** are sufficiently different to the known probes **A** that it was not certain that these would also bind

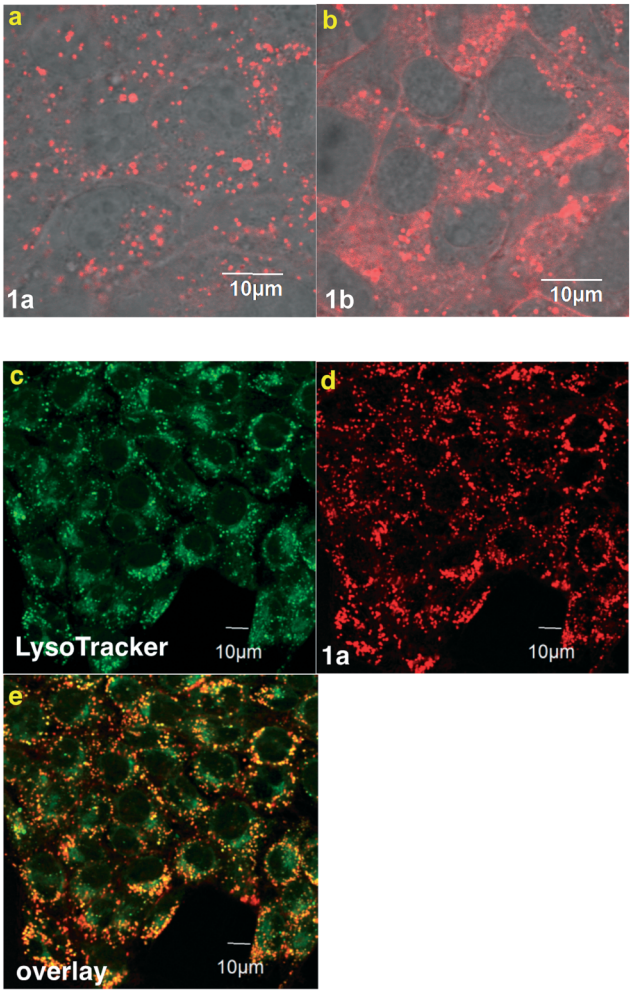

Fig. 3 Imaging with 4T1 cells. a Probe **1a** was internalized; whereas, b much more of **1b** accumulated in the cell walls (overlay images of fluorescent probes and bright field imaging). c LysoTracker and probe **1a** (d) colocalized as shown in e.

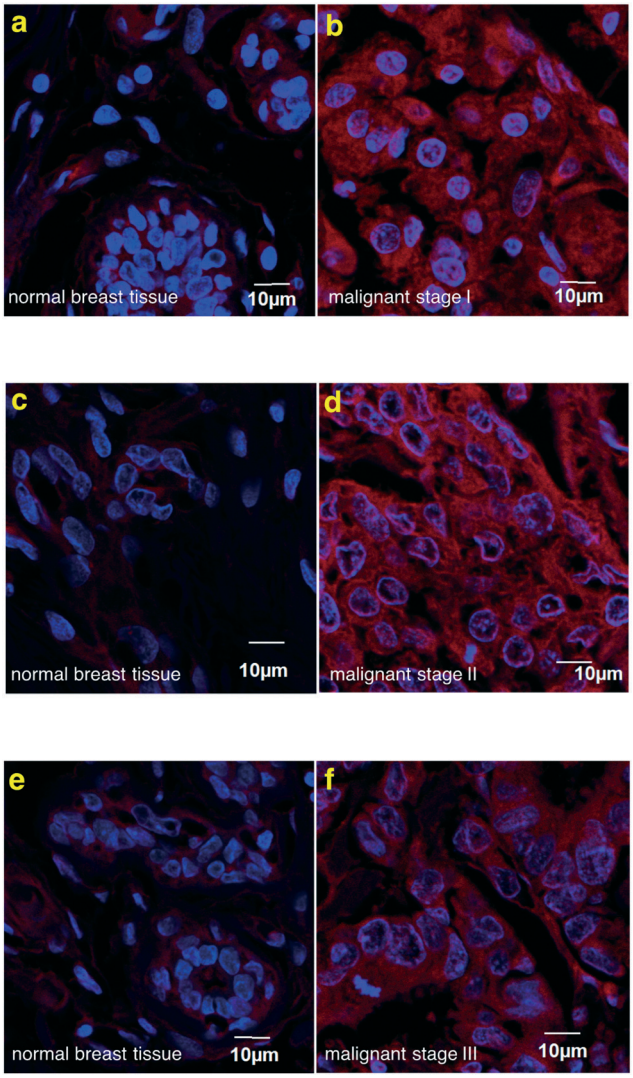

Fig. 4 Histochemistry on human breast tissue array. Probe **1a** stained on breast cancer tissue (b, d, f) much brighter than matched adjacent breast tissue control (a, c, e), (example from 3 cases).

TrkC. In the event, **1a** was selectively internalized into TrkC expressing cells, and stained human metastatic breast tumor tissues from cancer patients. *In vivo*, **1a** accumulated in a TrkC-expressing (4T1) breast cancer tumor model to a much higher degree than the isomeric control that does not bind TrkC (**1a-control**). Accumulation of both **1a** and **1a-control** in the liver was also observed, but this is to be expected for such a lipophilic compound (aza-BODIPY cores are very hydrophobic). The key probe **1a** did not accumulate in other organs to any extent that would preclude optical imaging of a primary breast cancer tumor.

Materials and methods

Cell culture and imaging

Murine breast cancer 4T1 cells were obtained from American Type Culture Collection and cultured in Dulbecco's modified Eagle's medium (DMEM) containing 10% fetal bovine serum (FBS) at 37 °C in humidified atmosphere with 5% CO_2. Subcellular localization was measured on living 4T1 cells using an Olympus FV1000 Confocal Microscope. Throughout, digital images were captured with a 100×/1.4 oil objective with the following filter sets: for LysoTracker Green: excitation 488 nm; for probes **1a** and **1b**: excitation 633 nm. Sequential optical sections (Z-stacks) from the basal-to-apical surfaces of the cell were also acquired.

Intracellular localization

4T1 cells were incubated with **1a**, 1 μM, for 12 h at 37 °C. After the cells were washed with PBS, LysoTracker Green (Life Technology, 500 nM) was added and the cells were incubated for 30 min at 37 °C. The cells were washed again with PBS before imaging.

Histochemistry

Two slides of human breast cancer tissue microarrays (BRC962) containing 36 cases of breast cancers and 12 cases

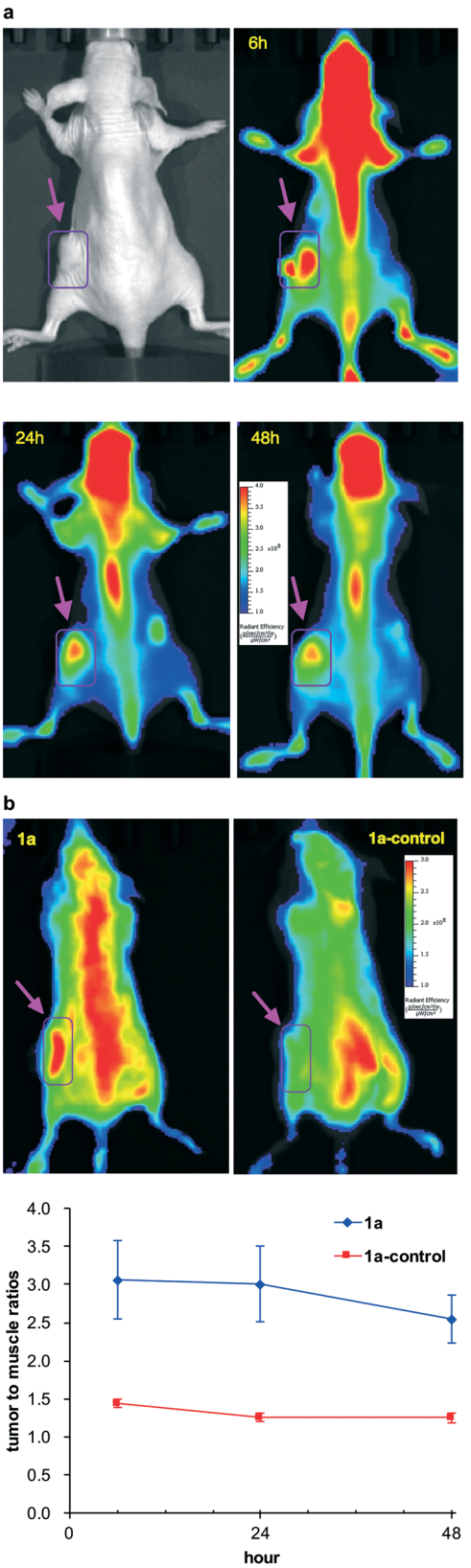

Fig. 5 a *In vivo* NIR fluorescence images (at 6 h, 24 h, and 48 h p.i.) of 4T1 tumor-bearing mice injected (iv) with **1a**. Arrows indicate the tumors. b Representative NIR fluorescent images of mice injected with **1a** (left) or **1a-control** compound at 48 h p.i. (right). The arrows indicate the tumors (top); an ROI study of tumor/normal tissue (muscle) ratio of **1a** and **1a-control** in the imaging groups (n = 3).

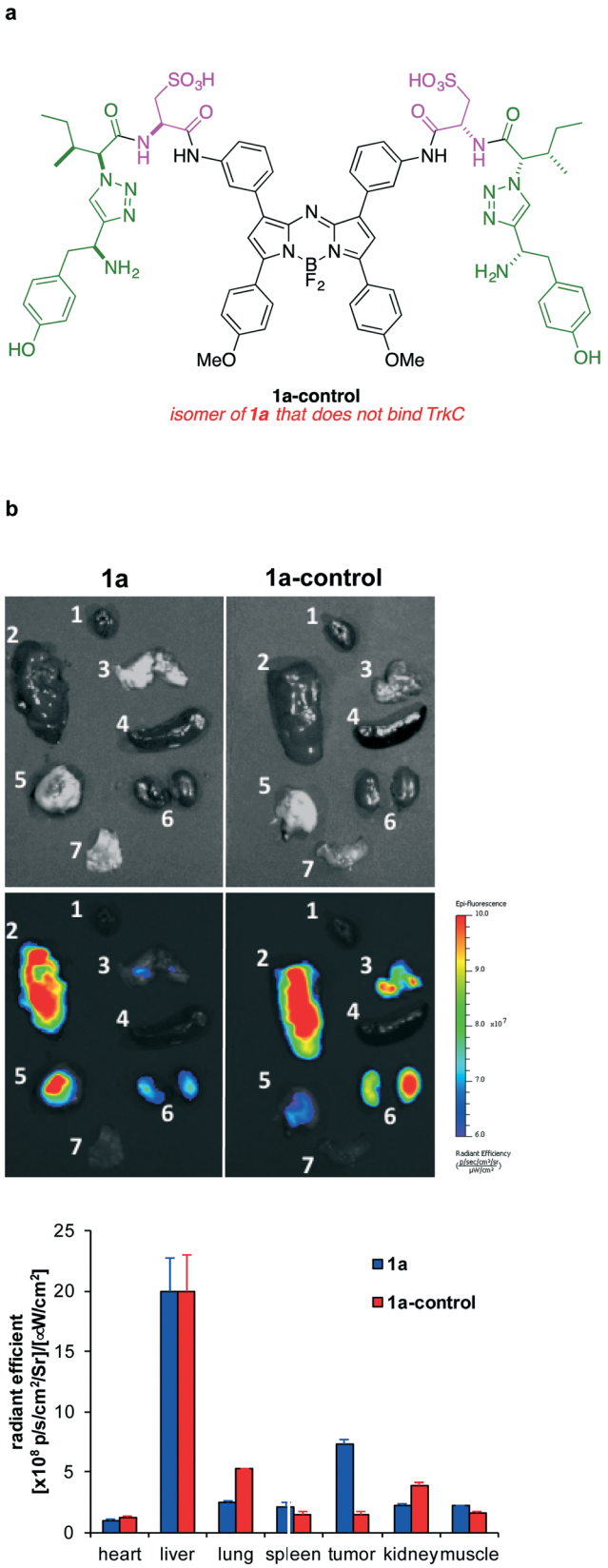

Fig. 6 a Structure of **1a-control**. b Representative *ex vivo* fluorescent images of organs (1 heart, 2 liver, 3 lungs, 4 spleen, 5 tumor, 6 kidneys, 7 muscle) collected from the mice injected with **1a** and **1a-control** at 48 h p.i.; and, quantification of fluorescence in those organs (n = 3).

of normal, reactive and benign tumour tissues of the breast in duplicates were purchased from US Biomax, Inc. **1a** and anti-TrkC antibody – N-terminal (ab188592, Abcam U.S.A.) were used as staining materials and the histology protocol was performed according to a published procedure.[42] All tissues were visualized using an Olympus FV1000 confocal microscope.

Animal model

Murine breast cancer 4T1 cells were obtained from American Type Culture Collection and cultured in Dulbecco's modified Eagle's medium (DMEM) containing 10% fetal bovine serum (FBS) at 37 °C in humidified atmosphere with 5% CO_2. Animal procedures were performed according to a protocol approved by Houston Methodist Research Institute Animal Care and Use Committee. Murine 4T1 cells (5×10^6) were suspended in 100 μL PBS and injected orthotopically into the lower left mammary fat pad of 6 weeks female BALB/c nu/nu mice (Charles River). Mice were subjected to the *in vivo* imaging studies when tumors reached 8–10 mm in diameter.

In vivo fluorescence imaging and *ex vivo* biodistribution study

In vivo and *ex vivo* fluorescence imaging was performed with IVIS200 imaging system, and quantified by Living Imaging software (Xenogen, CA). Excitation and emission filters were set at 640 nm and 680 nm respectively as suggested by the system for image acquisition. For *in vivo* studies (n = 3), stock solutions (~1 mM) of **1a** and **1a-control** conjugate in DMSO was diluted with PBS for injection. Each tumor-bearing mouse was injected intravenously with 10 nmol of **1a**. Images were acquired at 6 h, 24 h and 48 h post-injection (p.i.). For control studies (n = 3), mice were injected with 10 nmol of **1a-control** following the same procedures described above. Regions of interest (ROI) were drawn over the tumor and adjacent normal tissue to calculate the *in vivo* tumor/normal tissue ratio. In the ROI analysis, mean fluorescence intensities of the tumor area (tumor) defined as fluorescent radiant efficiency and of the area at the adjacent normal tissue (muscle) were calculated. After the 48 h imaging, mice were sacrificed, and tumors, muscles and major organs (*i.e.*, heart, lung, liver, spleen and kidney) were excised for *ex vivo* imaging acquisition. ROI analysis and quantification of the fluorescence signals (n = 3) were performed with Living Imaging (Xenogen, CA).

Notes

The authors declare no competing financial interests.

Conflicts of interest

The authors declare no competing interests.

Acknowledgements

We thank DoD BCRP Breakthrough Award (BC141561), CPRIT (RP150559 and RP170144), The Robert A. Welch Foundation (A-1121), and High Impact Research (HIR (UM.C/625/1/HIR/MOHE/MED/17 & UM.C/625/1/HIR/MOHE/MED/33) from the Ministry of Higher Education, Malaysia, for financial support. The NMR instrumentation at Texas A&M University was supported by a grant from the National Science Foundation (DBI-9970232) and the Texas A&M University System. The Olympus FV1000 confocal microscope acquisition was supported by the Office of the Vice President for Research at Texas A&M University. We thank the preclinical imaging core facility of Houston Methodist Research Institute for imaging support. Procedures for animal housing, maintenance, and euthanization were performed according to the American Veterinary Medical Association guidelines, and the IACUC approval from Methodist Hospital.

References

1 A. Patapoutian and L. F. Reichardt, *Curr. Opin. Neurobiol.*, 2001, **11**, 272–280.
2 E. J. Huang and L. F. Reichardt, *Annu. Rev. Biochem.*, 2003, **72**, 609–642.
3 M. V. Chao, *Nat. Rev. Neurosci.*, 2003, **4**, 299–309.
4 L. Tessarollo, P. Tsoulfas, D. Martin-Zanca, D. J. Gilbert, N. A. Jenkins, N. G. Copeland and L. F. Parada, *Development*, 1993, **118**, 463–475.
5 M. Ryden, R. Sehgal, C. Dominici, F. H. Schilling, C. F. Ibanez and P. Kogner, *Br. J. Cancer*, 1996, **74**, 773–779.
6 D. J. Yamashiro, A. Nakagawara, N. Ikegaki, X. G. Liu and G. M. Brodeur, *Oncogene*, 1996, **12**, 37–41.
7 G. M. Brodeur, A. Nakagawara, D. J. Yamashiro, N. Ikegaki, X. G. Liu, C. G. Azar, C. P. Lee and A. E. Evans, *J. Neuro-Oncology*, 1997, **31**, 49–55.
8 D. J. Yamashiro, X. G. Liu, C. P. Lee, A. Nakagawara, N. Ikegaki, L. M. McGregor, S. B. Baylin and G. M. Brodeur, *Eur. J. Cancer*, 1997, **33**, 2054–2057.
9 M. Encinas, M. Iglesias, N. Llecha and J. X. Comella, *J. Neurochem.*, 1999, **73**, 1409–1421.
10 M. A. Grotzer, A. J. Janss, K. M. Fung, J. A. Biegel, L. N. Sutton, L. B. Rorke, H. Zhao, A. Cnaan, P. C. Phillips, V. M. Y. Lee and J. Q. Trojanowski, *J. Clin. Oncol.*, 2000, **18**, 1027–1035.
11 M. E. Evangelopoulos, J. Weis and A. Kruttgen, *J. Neuro-Oncology*, 2004, **66**, 101–110.
12 P. Laneve, L. Di Macrotullio, U. Gioia, M. E. Fiori, E. Ferretti, A. Gulino, I. Bozzoni and E. Caffarelli, *Proc. Natl. Acad. Sci. U. S. A.*, 2007, **104**, 7957–7962.
13 G. M. Brodeur, J. E. Minturn, R. Ho, A. M. Simpson, R. Iyer, C. R. Varela, J. E. Light, V. Kolla and A. E. Evans, *Clin. Cancer Res.*, 2009, **15**, 3244–3250.
14 M. Bassili, E. Birman, N. F. Schor and H. U. Saragovi, *Cancer Chemother. Pharmacol.*, 2010, **65**, 1047–1056.
15 L. Harel, B. Costa and M. Fainzilber, *Dev. Neurobiol.*, 2010, **70**, 298–303.

16 V. Bernard-Gauthier, A. Aliaga, A. Aliaga, M. Boudjemeline, R. Hopewell, A. Kostikov, P. Rosa-Neto, A. Thiel and R. Schirrmacher, *ACS Chem. Neurosci.*, 2015, **6**, 260–276.
17 S. Kumar and J. de Vellis, *J. Neurosci. Res.*, 1996, **44**, 490–498.
18 Y. Wang, C. Hagel, W. Hamel, S. Muller, L. Kluwe and M. Westphal, *Acta Neuropathol.*, 1998, **96**, 357–364.
19 C. Calatozzolo, A. Salmaggi, B. Pollo, F. L. Sciacca, M. Lorenzetti, A. Franzini, A. Boiardi, G. Broggi and C. Marras, *Neurol. Sci.*, 2007, **28**, 304–310.
20 M. Assimakopoulou, M. Kondyli, G. Gatzounis, T. Maraziotis and J. Varakis, *BMC Cancer*, 2007, **7**, 202–210.
21 S. Lawn, A. Chan Jennifer, N. Krishna, A. Pisklakova, X. Qu, A. Fenstermacher David, M. Fournier, D. Vrionis Frank, N. Tran, S. Kenchappa Rajappa and A. Forsyth Peter, *J. Biol. Chem.*, 2014, **290**, 3814–3824.
22 P. Stephens, S. Edkins, H. Davies, C. Greenman, C. Cox, C. Hunter, G. Bignell, J. Teague, R. Smith, C. Stevens, S. O'Meara, A. Parker, P. Tarpey, T. Avis, A. Barthorpe, L. Brackenbury, G. Buck, A. Butler, J. Clements, J. Cole, E. Dicks, K. Edwards, S. Forbes, M. Gorton, K. Gray, K. Halliday, R. Harrison, K. Hills, J. Hinton, D. Jones, V. Kosmidou, R. Laman, R. Lugg, A. Menzies, J. Perry, R. Petty, K. Raine, R. Shepherd, A. Small, H. Solomon, Y. Stephens, C. Tofts, J. Varian, A. Webb, S. West, S. Widaa, A. Yates, F. Brasseur, C. S. Cooper, A. M. Flanagan, A. Green, M. Knowles, S. Y. Leung, L. H. J. Looijenga, B. Malkowicz, M. A. Pierotti, B. Teh, S. T. Yuen, A. G. Nicholson, S. Lakhani, D. F. Easton, B. L. Weber, M. R. Stratton, P. A. Futreal and R. Wooster, *Nat. Genet.*, 2005, **37**, 590–592.
23 S. V. Ivanov, A. Panaccione, B. Brown, Y. Guo, C. A. Moskaluk, M. J. Wick, J. L. Brown, A. V. Ivanova, N. Issaeva, A. K. El-Naggar and W. G. Yarbrough, *Oncogene*, 2013, **32**, 3698–3710.
24 W. Jin, G.-M. Kim, M.-S. Kim, M.-H. Lim, C.-H. Yun, J. Jeong, J.-S. Nam and S.-J. Kim, *Carcinogenesis*, 2010, **31**, 1939–1947.
25 W. Jin, C. Yun, M. K. Kwak, T. A. Kim and S. J. Kim, *Oncogene*, 2007, **26**, 7684–7691.
26 W. Jin, C. Yun, J. Jeong, Y. Park, H.-D. Lee and S.-J. Kim, *J. Biol. Chem.*, 2008, **283**, 1391–1400.
27 M. J. Blasco-Gutierrez, I. J. San Jose-Crespo, E. Zozaya-Alvarez, R. Ramos-Sanchez and N. Garcia-Atares, *Cancer Invest.*, 2007, **25**, 405–410.
28 H. Hondermarck, *Cytokine Growth Factor Rev.*, 2012, **23**, 357–365.
29 X. Xu, S. R. Tahan, T. L. Pasha and P. J. Zhang, *J. Cutaneous Pathol.*, 2003, **30**, 318–322.
30 A. Marconi, M. Terracina, C. Fila, J. Franchi, F. Bonte, G. Romagnoli, R. Maurelli, C. M. Failla, M. Dumas and C. Pincelli, *J. Invest. Dermatol.*, 2003, **121**, 1515–1521.
31 D. Marchetti, B. Murry, J. Galjour and A. Wilke-Greiter, *J. Cell. Biochem.*, 2003, **88**, 865–872.
32 M. J. C. Hendrix, E. A. Seftor, D. A. Kirschmann, V. Quaranta and R. E. B. Seftor, *Ann. N. Y. Acad. Sci.*, 2003, **995**, 151–161.
33 A. Marconi, M. C. Panza, M. Bonnet-Duquennoy, K. Lazou, R. Kurfurst, F. Truzzi, R. Lotti, G. De Santis, M. Dumas, F. Bonte and C. Pincelli, *Int. J. Cosmet. Sci.*, 2006, **28**, 255–261.
34 F. Truzzi, A. Marconi, R. Lotti, K. Dallaglio, L. E. French, B. L. Hempstead and C. Pincelli, *J. Invest. Dermatol.*, 2008, **128**, 2031–2040.
35 V. A. Botchkarev, M. Yaar, E. M. J. Peters, S. P. Raychaudhuri, N. V. Botchkareva, A. Marconi, S. K. Raychaudhuri, R. Paus and C. Pincelli, *J. Invest. Dermatol.*, 2006, **126**, 1719–1727.
36 D. Marchetti, Y. Denkins, J. Reiland, A. Greiter-Wilke, J. Galjour, B. Murry, J. Blust and M. Roy, *Pathol. Oncol. Res.*, 2003, **9**, 147–158.
37 Y. Denkins, J. Reiland, M. Roy, N. D. Sinnappah-Kang, J. Galjour, B. P. Murry, J. Blust, R. Aucoin and D. Marchetti, *Neuro-Oncology*, 2004, **6**, 154–165.
38 A. Vaishnavi, T. Le Anh and C. Doebele Robert, *Cancer Discovery*, 2015, **5**, 25–34.
39 F. Truzzi, A. Marconi and C. Pincelli, *Derm.-Endocrinol.*, 2011, **3**, 32–36.
40 L. Dolle, E. Adriaenssens, I. E. Yazidi-Belkoura, X. L. Bourhis, V. Nurcombe and H. Hondermarck, *Curr. Cancer Drug Targets*, 2004, **4**, 463–470.
41 V. Bernard-Gauthier, M. Boudjemeline, P. Rosa-Neto, A. Thiel and R. Schirrmacher, *Bioorg. Med. Chem.*, 2013, **21**, 7816–7829.
42 S. C. Kue, A. Kamkaew, H. B. Lee, L. L. Chung, L. V. Kiew and K. Burgess, *Mol. Pharmaceutics*, 2015, **12**, 212–222.
43 A. Kamkaew, H. Lim Siang, B. Lee Hong, V. Kiew Lik, Y. Chung Lip and K. Burgess, *Chem. Soc. Rev.*, 2012, **42**, 77–88.
44 S. G. Awuah and Y. You, *RSC Adv.*, 2012, **2**, 11169–11183.
45 R. Ziessel, C. Goze and G. Ulrich, *Synthesis*, 2007, **6**, 936–949.
46 A. Loudet and K. Burgess, BODIPY Dyes and Their Derivatives: Syntheses and Spectroscopic Properties, *Handbook of Porphyrin Science: With Applications to Chemistry, Physics, Materials Science, Engineering, Biology and Medicine*, ed. K. Kadish, K. Smith and R. Guilard, World Scientific, 2010, p. 203.
47 H. Lu, J. Mack, Y. Yang and Z. Shen, *Chem. Soc. Rev.*, 2014, **43**, 4778–4823.
48 Y. Angell, D. Chen, F. Brahimi, H. U. Saragovi and K. Burgess, *J. Am. Chem. Soc.*, 2008, **130**, 556–565.
49 A. Kamkaew and K. Burgess, *Chem. Commun.*, 2015, **51**, 10664–10667.
50 M. Meldal and C. W. Tornoe, *Chem. Rev.*, 2008, **108**, 2952–3015.
51 P. Wu and V. V. Fokin, *Aldrichimica Acta*, 2007, **40**, 7–17.
52 G. A. Johnson, N. Muthukrishnan and J.-P. Pellois, *Bioconjugate Chem.*, 2013, **24**, 114–123.
53 R. A. Segal, *Annu. Rev. Neurosci.*, 2003, **26**, 299–330.